

Supporting Information for:

Electronic Structure of $\text{PbCr}_{(1-x)}\text{S}_x\text{O}_4$ Solid Solution: an Inside Look at Van Gogh Yellow Degradation

Ana B. Muñoz-García,* Arianna Massaro, and Michele Pavone.

Department of Chemical Sciences, University of Naples Federico II, Via Cintia 21, 80126 Naples, Italy.

S.1. Structural models for VGY

$\text{PbCr}_{(1-x)}\text{S}_x\text{O}_4$ is a solid solution with ABO_4 general formula: A-sites are occupied by Pb and B-sites by Cr and S in different ratio. PbCrO_4 ($x=0$) presents two phases, monoclinic (M) and orthorhombic (O): M is the most abundant and belongs to $P21/n$ space group; O has been detected in small percentages and belongs to the $Pnma$ one.^{S1} Also PbSO_4 ($x=1$) belongs to the orthorhombic $Pnma$ space group. In all these cases, the unit cell contains four formula units ($\text{A}_4\text{B}_4\text{O}_{16}$) for a total of 24 atoms (Figure S.1.0). In M, every PbCrO_4 atom (Pb, Cr, OI, OII, OIII and OIV) occupies 4e Wyckoff sites.^{S2} In O crystals, Pb, Cr/S, OI and OII occupy 4c Wyckoff positions and OIII atoms are in 8d ones.^{S3,S4}

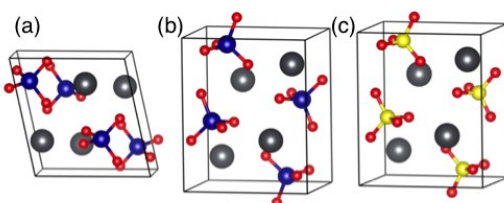


Figure S.1.0. Structural models for lead chromate (a) monoclinic and (b) orthorhombic unit cells and for (c) orthorhombic lead sulfate. Spheres represent atoms, color legend: Pb grey, Cr blue, S yellow, and O red.

Besides pure lead chromate and sulphate (see main text for structural details), we have explored the $\text{PbCr}_{(1-x)}\text{S}_x\text{O}_4$ solid solution with $x=0.125, 0.25, 0.50, 0.75$ and 0.875 . In the following, we describe the corresponding structural models.

- **$\text{PbCr}_{0.875}\text{S}_{0.125}\text{O}_4$:** The 24-atom ABO_4 unit cell is insufficient to describe the 7:1 Cr:S ratio. Thereby, a supercell approach is needed in order to get the stoichiometric formula: we substituted 1 Cr atom with 1 S atom in monoclinic 48-atom $2 \times 1 \times 1$ PbCrO_4 and orthorhombic $1 \times 2 \times 1$ PbCrO_4 supercells. Figure S.1.1 shows the relaxed structure of the two models.

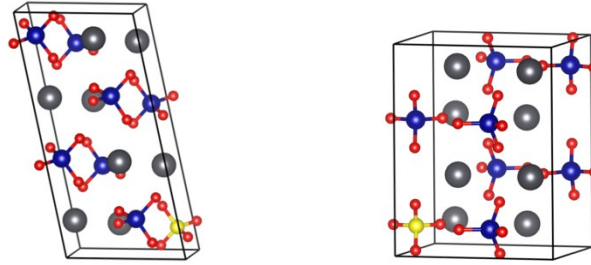


Figure S.1.1 Structural models of monoclinic (left) and orthorhombic (right) $\text{PbCr}_{0.875}\text{S}_{0.125}\text{O}_4$

- **$\text{PbCr}_{0.75}\text{S}_{0.25}\text{O}_4$** : it presents a 3:1 Cr:S ratio, which can be modeled by substitution of 1 Cr atom by 1 S atom in the 24-atom ABO_4 cell (Figure S.1.2)

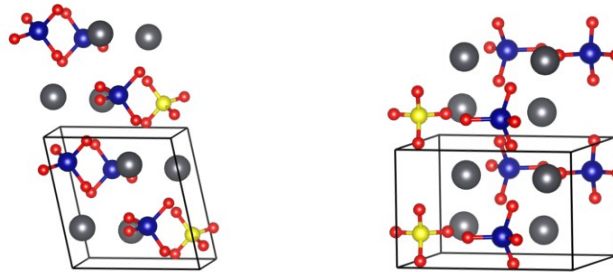


Figure S.1.2 Structural models of monoclinic (left) and orthorhombic (right) $\text{PbCr}_{0.75}\text{S}_{0.25}\text{O}_4$

- **$\text{PbCr}_{0.50}\text{S}_{0.50}\text{O}_4$** : we have modeled the 1:1 Cr:S ratio by substituting 2 out of 4 Cr atoms in the 24-atom ABO_4 unit cell by S. Depending on the relative position of the two substituents in the unit cell, three different configurations arise (Figs S.1.3-5):
 - **Configuration A**, with the largest distance between the 2 S atoms:

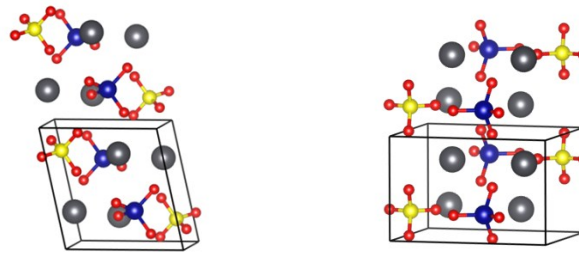


Figure S.1.3 Structural models of monoclinic (left) and orthorhombic (right) $\text{PbCr}_{0.50}\text{S}_{0.50}\text{O}_4$ (configuration A)

- **Configuration B**, with the smallest S – S distance:

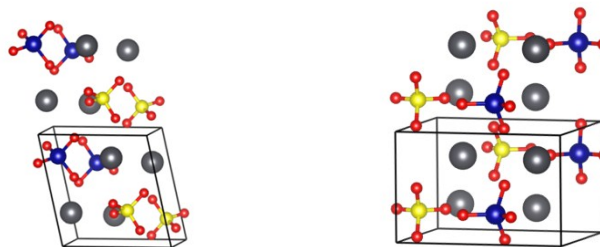


Figure S.1.4 Structural models of monoclinic (left) and orthorhombic (right) $\text{PbCr}_{0.50}\text{S}_{0.50}\text{O}_4$ (configuration B)

- **Configuration C**, with an intermediate S – S distance:

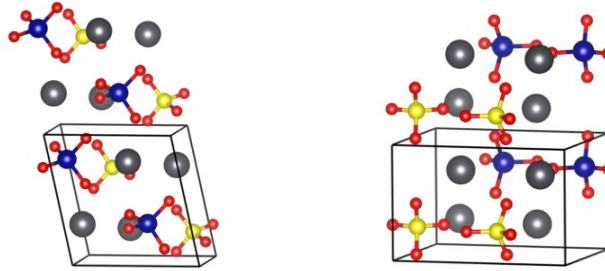


Figure S.1.5 Structural models of monoclinic (left) and orthorhombic (right) $\text{PbCr}_{0.50}\text{S}_{0.50}\text{O}_4$ (configuration C)

- **$\text{PbCr}_{0.25}\text{S}_{0.75}\text{O}_4$** : This lattice presents a 1:3 Cr:S ratio, which can be, in principle modeled with the 24-atom ABO_4 unit. Since this particular solid solution with 1:3 Cr:S ratio is not found experimentally (see main text for details), we have focused on it for analysing the thermodynamic stability of the solid solution and we have considered 48-atom supercells in order to evaluate multiple spatial configurations within the Cr/S sublattice. We substituted 6 Cr atoms with 6 S atoms in $2 \times 1 \times 1$ monoclinic and $1 \times 2 \times 1$ orthorhombic supercells. Figure S.1.6 shows random configuration among the 7 possible configurations for each space group.

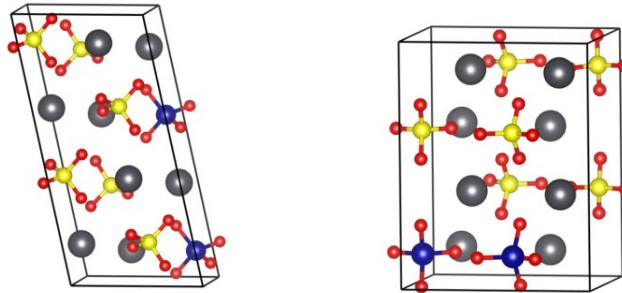


Figure S.1.6 Structural models of monoclinic (left) and orthorhombic (right) $\text{PbCr}_{0.25}\text{S}_{0.75}\text{O}_4$

- **$\text{PbCr}_{0.125}\text{S}_{0.875}\text{O}_4$** : as for $\text{PbCr}_{0.875}\text{S}_{0.125}\text{O}_4$, we have modeled the 1:7 Cr:S ratio by substitution of 7 Cr atoms with 7 S atoms in 48-atoms supercells (Fig. S.1.7)

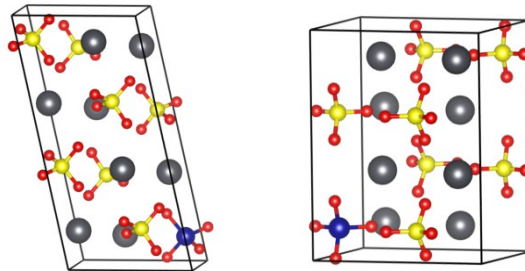


Figure S.1.8 Structural models of monoclinic (left) and orthorhombic (right) $\text{PbCr}_{0.125}\text{S}_{0.875}\text{O}_4$

S.2. Equilibrium Structures: PBE vs PBE-D3 lattice constants and Monoclinic vs Orthorhombic cell volumes

Table S.2.1 gathers the equilibrium lattice constants obtained with PBE and PBE-D3(BJ) methods, in comparison with experimental values.

Table S.2.1 Comparison between experimental lattice parameters and PBE/PBE – D3 (BJ) equilibrium structures. For PbCrO_4 (monoclinic): $\beta=102.40^\circ$ (experimental), $\beta=102.54^\circ$ (theoretical). *Data without experimental counterpart

Level of theory		Lattice parameters (\AA)					
		Monoclinic $P2_1/n$			Orthorhombic $Pnma$		
		<i>a</i>	<i>b</i>	<i>c</i>	<i>a</i>	<i>b</i>	<i>c</i>
PbCrO_4	<i>Experimental</i> [Ref. 1]	7.128	7.437	6.801	8.667	5.548	7.118
	PBE	7.274	7.605	6.912	8.712	5.617	7.165
	PBE-D3(BJ)	7.131	7.513	6.809	8.647	5.575	7.111
PbSO_4	<i>Experimental</i> [Ref. 2]	-	-	-	8.482	5.398	6.959
	PBE	(7.070)	7.285	6.755)*	8.528	5.530	7.057
	PBE-D3(BJ)	(7.054)	7.269	6.740)*	8.489	5.419	7.047

Ref 1. Monico L., Janssens K., Hendriks E., Brunetti B.G., Miliani C., *J. Raman. Spectrosc.*, **45**, 1034-45, (2014)

Ref 2. Miyake M., Minato I., Morikawa H., Iwai S., *Am. Mineral.*, **63**, 506-510, (1978)

Table S.2.2 lists the equilibrium volumes of monoclinic and orthorhombic at PBE-D3(BJ) level of theory.

Table S.2.2 Calculated equilibrium volumes of monoclinic and orthorhombic VGY solid solution at PBE-D3 level of theory. In parenthesis, forms that are not detected experimentally.

Structure	Equilibrium Volume (\AA^3)	
	Monoclinic $P2_1/n$	Orthorhombic $Pnma$
PbCrO_4	356.12	342.85
$\text{PbCr}_{0.875}\text{S}_{0.125}\text{O}_4$	354.69	(353.98)
$\text{PbCr}_{0.75}\text{S}_{0.25}\text{O}_4$	352.62	(351.92)
$\text{PbCr}_{0.50}\text{S}_{0.50}\text{O}_4$	347.90	(344.95)
$\text{PbCr}_{0.125}\text{S}_{0.875}\text{O}_4$	(352.53)	333.96
PbSO_4	(337.51)	324.17

S.3. Exploring segregation in VGY

We have hypothesized a possible tendency towards phase separation between lead chromate and lead sulphate already in the bulk state as a first cause of the degradation.

Sulphur segregation has been simulated by optimization of the three different configurations of $\text{PbCr}_{0.50}\text{S}_{0.50}\text{O}_4$ solid solution described in S.1. Among these structures, it is possible to distinguish between a more segregated (smallest distance between sulphur atoms, B), a more homogeneous structure (largest S–S distance, structure A) and an intermediate situation (configuration C). Fig. S.3 shows the energy differences with respect to the most stable configuration after relaxation.

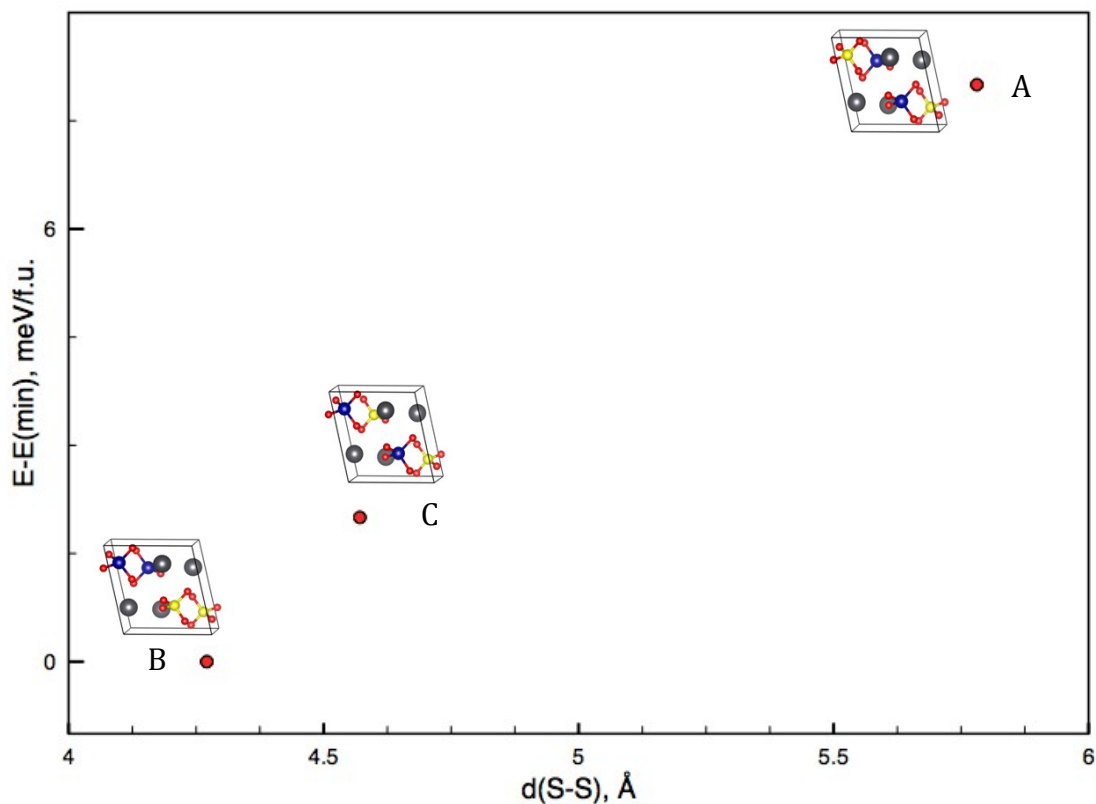


Figure S.3 Difference in energy ($E - E_{(\text{min})}$) of each $\text{PbCr}_{0.50}\text{S}_{0.50}\text{O}_4$ configuration (see S.1. for details) compared with the minimum-energy configuration as a function of S – S distance.

From our calculations, we can state that the “segregated” configuration B is the most stable, while the “homogeneous” solution A is the less stable. One reason behind this tendency of atoms at the B site of the ABO_4 structure to aggregate can be found in the significant difference between Cr-O and S-O distances (~ 1.66 and 1.49 Å, respectively, in both the parent solids and in VGY with $x = 0.5$), that brings an important size mismatch among the BO_4 moieties. The overall stress on the bulk structure is minimized when the dissimilar moieties are close in the cell.

S.4. Bader (AIM) Charge analysis of PbCrO_4

Table S.4 gathers the calculated Bader charges of Pb, Cr and O species in monoclinic PbCrO_4 , which give a qualitative indication of their oxidation state in this solid. From our calculations, Pb presents a oxidation state close to the +2 formal oxidation state for A-site

in ABO_4 compounds. Cr and O oxidation states, however, are very far from the formal +6 and -2 expected, which is a clear indication of the high degree of covalency of Cr-O bonds. Thus, $PbCrO_4$ can be regarded as $(CrO_4)^{2-}$ highly moieties electrostatically attracted to Pb^{2+} cations. For this reason, it is reasonable to describe Cr, not as Cr(IV) with d^0 configuration, but with some occupation at the d orbitals, which hybridize with oxygen p orbitals.

Table S.4 Calculated Bader charges of Pb, Cr and O in monoclinic $PbCrO_4$ at PBE and PBE+U levels of theory

Specie	Bader Charges		
	Formal	PBE	PBE+U ($U-J_{Cr}=3.2$ eV)
Pb	+2	+1.544	+1.542
Cr	+6	+1.820	+1.828
O	-2	-0.816	-0.818

S.5. PBE(+U) bandgaps in VGY

Table S.5 lists the calculated eigenvalue gaps of the VGY solid solution at the PBE and PBE+U levels of theory. The PBE+U values have been used to estimate the G_0W_0 -related bandgaps according to eq. 3 of the main text.

Table S.5 Band gaps of $PbCr_{(1-x)}S_xO_4$ equilibrium structures at PBE and PBE+U levels of theory

Structure	Band gap (eV)			
	<i>Monoclinic P2₁/n</i>		<i>Orthorhombic Pnma</i>	
	PBE	PBE+U	PBE	PBE+U
$PbCrO_4$	1.68	1.89	1.95	2.16
$PbCr_{0.875}S_{0.125}O_4$	1.73	1.94	1.98	2.19
$PbCr_{0.75}S_{0.25}O_4$	1.85	2.05	2.05	2.26
$PbCr_{0.50}S_{0.50}O_4$	A	1.92	2.12	2.06
	B	1.92	2.12	2.19
	C	1.94	2.13	2.18
$PbCr_{0.125}S_{0.875}O_4$	2.04	2.24	2.28	2.47
$PbSO_4$	4.36	-	4.03	-

S.6. PDOS of VGY solid solution

Figs. S.6.1, S.6.2 and S.6.3 display the computed projected density of states of $PbCr_{0.875}S_{0.125}O_4$, $PbCr_{0.75}S_{0.25}O_4$ and $PbCr_{0.5}S_{0.5}O_4$ (configuration B, the most stable – see S.3 for details), respectively. Together with that of $PbCr_{0.875}S_{0.125}O_4$ (see Fig. 8 in the main

text), they show that the electronic structure of VGY solid solution for all x retains the band edges features of PbCrO_4 (Fig. 6 in the main text), while S sites are very intern and do not participate in the band edges character.

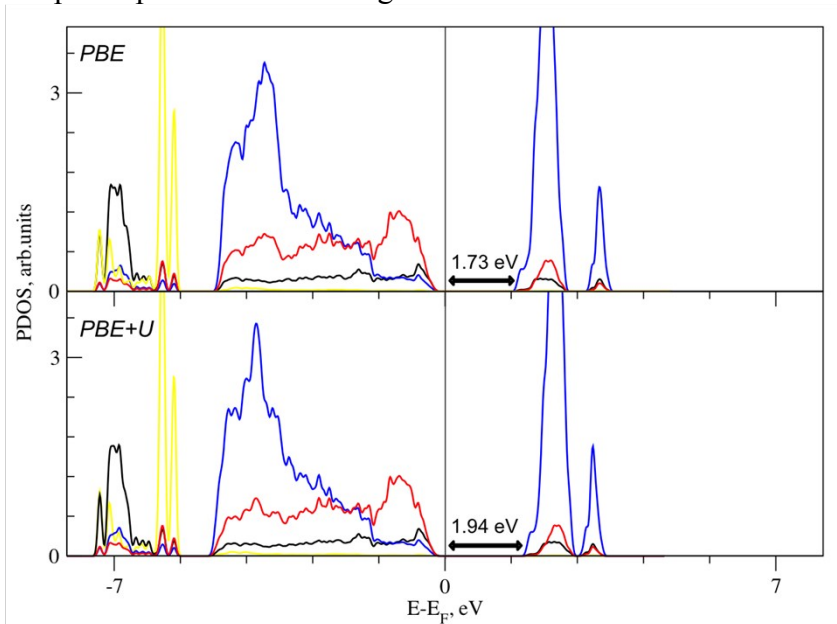


Figure S.6.1 Projected density of states (PDOS) of monoclinic $\text{PbCr}_{0.875}\text{S}_{0.125}\text{O}_4$ equilibrium structure at PBE and PBE+U levels of theory. Color legend: Pb d states are in black, Cr d states in blue, and O p states in red. The Fermi energy (E_F) is set to zero. Eigenvalue gaps are indicated (in eV).

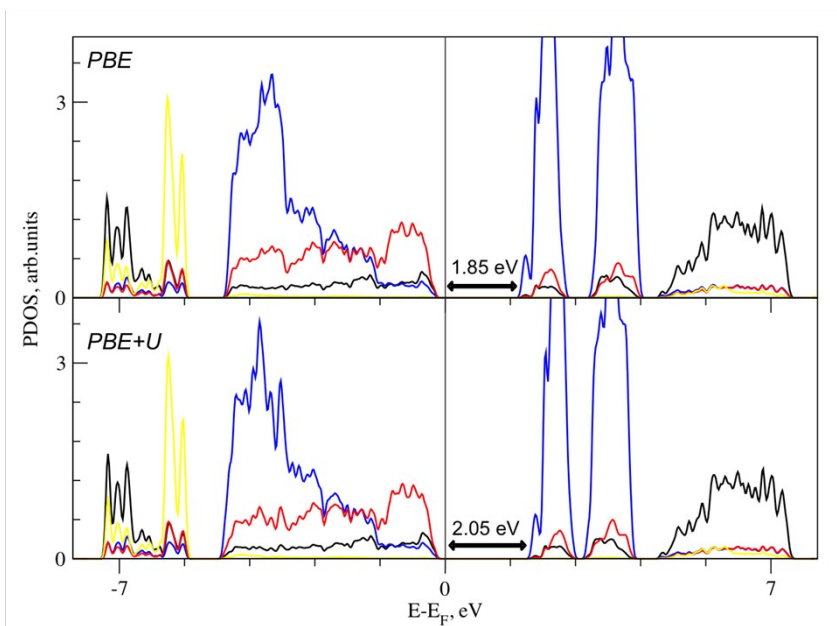


Figure S.6.2 Projected density of states (PDOS) of monoclinic $\text{PbCr}_{0.75}\text{S}_{0.25}\text{O}_4$ equilibrium structure at PBE and PBE+U levels of theory. Color legend: Pb d states are in black, Cr d states in blue, and O p states in red. The Fermi energy (E_F) is set to zero. Eigenvalue gaps are indicated (in eV).

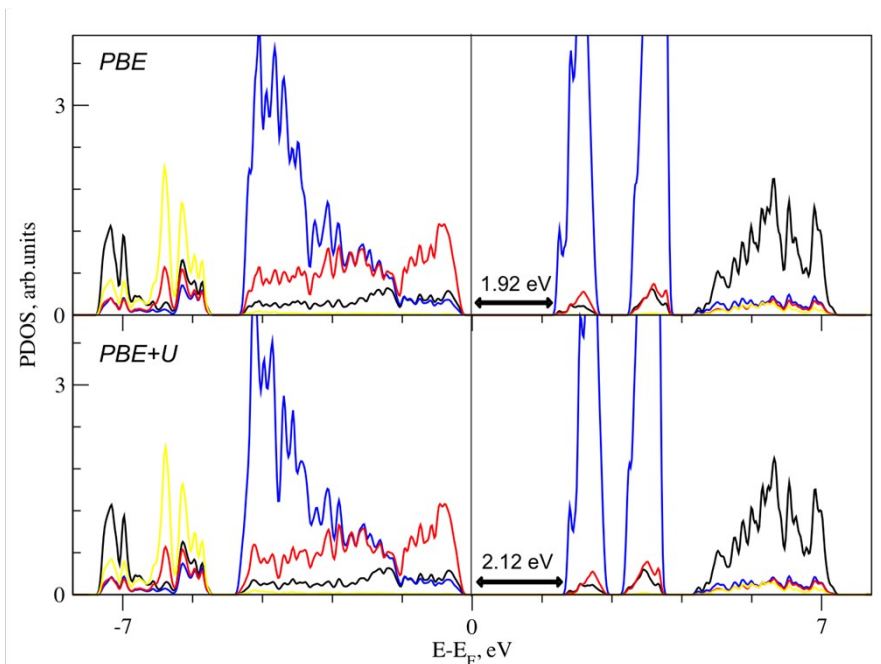


Figure S.6.3 Projected density of states (PDOS) of monoclinic $\text{PbCr}_{0.5}\text{S}_{0.5}\text{O}_4$ equilibrium structure (configuration B) at PBE and PBE+U levels of theory. Color legend: Pb d states are in black, Cr d states in blue, and O p states in red. The Fermi energy (E_F) is set to zero. Eigenvalue gaps are indicated (in eV).

REFERENCES

- S1. L. Monico, K. Janssens, E. Hendriks, B.G. Brunetti, C. Miliani, Raman study of different crystalline forms of PbCrO_4 and $\text{PbCr}_{1-x}\text{S}_x\text{O}_4$ solid solutions for the noninvasive identification of chrome yellows in paintings: a focus on works by Vincent van Gogh. *Journal of Raman Spectroscopy* **2014**, 45, 1034-1045.
- S2. E. Bandiello, D. Errandonea, D. Martinez-Garcia, D. Santamaria-Perez, F. J. Manjón, Effects of high-pressure on the structural, vibrational, and electronic properties of monazite-type PbCrO_4 , *Phys. Rev. B* **2012**, 85, 024108.
- S3. G. Collotti, L. Conti, M. Zocchi, The structure of the orthorhombic modification of lead chromate PbCrO_4 . *Acta Crystallographica* **1959**, 12, 416-416.
- S4. M. Miyake, I. M., H. Morikawa and S. Iwai, Crystal structures and sulphate force constants of barite, celestite, and anglesite. *American Mineralogist* **1978**, 63, 506-510.